



Experimental investigation on behavior of reinforced concrete interior beam column joints retrofitted with fiber reinforced polymers

Bhuiyan Mohammad Golam Kibria¹ · Fahim Ahmed¹ · Raquib Ahsan¹ · Mehedi Ahmed Ansary¹

Received: 15 February 2018 / Accepted: 14 October 2019 / Published online: 29 October 2019
© Springer Nature Switzerland AG 2019

Abstract

This experimental study is undertaken to study the behavior of RC interior beam-column joints which lack in shear reinforcement and strengthened by FRPs and additional tie bars. The samples are constructed with transverse beams and slab. Total eight models have been prepared of which three joints have been strengthened by carbon FRP (CFRP) fabrics, two joints have been strengthened by CFRP plates and one model has been strengthened by adding tie bar into the joint. The samples have been subjected to incremental cyclic loading provided by hydraulic jacks under constant axial or gravity load and their load-deformation behaviors have been measured by dial gauges and video extensometer. The behaviors of the strengthened joints are compared with the control models. The joints without shear reinforcement undergo brittle failure under cyclic loading. But their ductility increases with increased concrete strength. The joints strengthened by the CFRPs show better load bearing capacity with enhanced ductile behavior. Location of the plastic hinges shifts from column to beam in case of the joints strengthened by CFRP plates and fabrics. The joint strengthened by additional tie bar and micro-concrete undergo large rotational deformation before they fail. Joints strengthened by CFRP fabrics exhibit better ductility and strength than those of the joints retrofitted by CFRP plates and tie bars. Joints strengthened by CFRP plate exhibited high rotational stiffness and are effective in resisting the diagonal crack travelling to transverse beams.

Keywords Retrofitted joints · CFRP fabrics and plates · Load deflection responses

Introduction

Reinforced concrete buildings constructed before 70's were designed for gravity loads only and did not show adequate seismic performances (Bai et al. 2003; Sharma et al. 2010). Weaknesses in joints were identified as one of the main causes for poor seismic performance. To overcome this deficiencies first guidelines for reinforced concrete beam-column (BC) joints were published in United States in 1976 (ACI-352R-76 1976) followed by New Zealand in 1982 (NZS 3101:1982 1982). Therefore, buildings constructed before 1976 may have significant deficiencies in the joint regions (Bai et al. 2003). Due to poor design and detailing of the BC joints of these buildings, they may lead to a total or partial collapse due to an earthquake (Sezen 2012;

Prota et al. 2004). BC joints are subjected to large shear forces during seismic events; therefore, many experimental and analytical researches had been carried out in past few decades on the behavior of RC BC joints under seismic condition (Mayfield et al. 1971; Ichinose 1991). Various international codes (ACI 318, 318M-08, ACI 352R-02, ACI ASCE, Committee 352, FEMA 273, BNBC 1993) of practices had also been evolved and undergone periodic revisions to incorporate these research findings into practice.

In Bangladesh, many RC buildings had been constructed without seismic detailing in the BC joints before or even after the inception of BNBC (1993). Change in the types of occupancy is very common as residential buildings are frequently converted to commercial and industrial buildings; number of floors is increased without proper design analysis. These buildings are vulnerable to seismic hazard and need to be strengthened.

Conventional retrofitting methods are sometimes difficult due to the nature of occupancy, importance of the structure, economic value of the non-operational period and cost of the man and materials. FRPs, which have high strength

✉ Fahim Ahmed
fahim07ce@gmail.com

¹ Department of Civil Engineering, Bangladesh University of Engineering and Technology (BUET), Dhaka 1000, Bangladesh

to weight ratio, are suggested and are used as retrofitting materials in many countries of the world as these materials are easy to place, need minimum relocation of existing occupancy and retrofitting time is very short compared to other methods.

Sharma et al. (2010), Beydokhty and Shariatmadar (2016), Sezen (2012), Pantelides et al. (2000), Mahini and Rounagh (2007) strengthened the joints by FRP wrappings. Mukherjee and Joshi (2005), Obaidat et al. (2019) used FRP plates at the damaged BC joints and found increased the shear strength of the joint. Mahini and Rounagh (2007), Akguzel and Pampanin (2011), Sezen (2012), Zgür Yurdakul and Avşar (2015) conducted research on exterior joints where access to the joints was relatively easy and the existence of floor slab was not considered. Pohoryles et al. (2015) conducted experiment on exterior joints with slabs and found that slab has a significant impact on the global behavior due to stiff slab limiting rotation.

Mukherjee and Joshi (2005) carried out a study to investigate the behavior of RCC beam column (BC) joint with and without adequate shear reinforcement in the joint region. The specimens with adequate shear reinforcement and strengthened with FRPs exhibited higher dissipation of energy and ultimate deformation than controlled specimens. Non-ductile joints strengthened by FRP also exhibited better performance and their performance depends on the number of layers of FRP wrapping. Murshed (2011) carried out seismic analysis on eight soft story structures which were retrofitted with FRP wraps. It was found that seismic performance of the soft story structures can be improved by FRP wraps. Improve in the lateral strength was negligible due to wraps but ductility improvement was quite satisfactory.

Al-Musallam and Al-Salloum (2007), Shiohara and Kusahara (2010) and Li and Kai (2010) conducted research on the behavior of RC interior beam-column joints. These studies were conducted on interior joints which did not include transverse beams and slabs.

This study attempted to access the interior beam column joints with transverse beams on all four sides and monolithic floor slab. It also attempted to increase the shear strength of the joints by inserting CFRP plate into the beam-column joint, wrapping beam and columns by CFRP fabrics and inclusion of tie bar in the joint region. To investigate the behavior of the RC interior BC joints retrofitted by FRP plates, fabrics and tie bars, incremental cyclic loading were provided with constant axial load on to the test samples. Half scale models with transverse beams and slab had been constructed before strengthening the joints. Following parameters had been considered to investigate the behavior of the joints: (a) interior joints having different concrete strength, (b) interior joints strengthened by wrapping beams and columns by CFRP fabrics, (c) interior joints strengthened by inserting CFRP

plates, (d) INTERIOR joints strengthened by inserting tie bar in the joint and replacing concrete by micro-concrete. Total eight models had been constructed for the study as follows: (a) two control models designated as Con 1 and Con 2, (b) three models strengthened by CFRP fabrics designated as Fabrics 1, Fabrics 2 and Fabrics 3, (c) two models strengthened by CFRP plate designated as Plate 1 and Plate 2, (d) one model strengthened by additional tie bar and micro-concrete mixture designated as MCS 1.

The outcome of the study will unveil the behavior of the strengthened RC interior BC joints and compare the behavior with the joints which lack in shear reinforcement. The research will also facilitate in developing methods of determining strength of retrofitted joints and identify suitable procedures to retrofit interior BC joints by CFRPs.

Detailing of control and test models

The models had been selected considering a typical full scale six storied RC Frame Structured Building. The building was analyzed as per BNBC (1993). An interior joint at the mid height of the structure had been selected for the experimental program. Considering the existing laboratory set up a half scale model had been finally selected. Total eight models were constructed for the experiment. All the models had identical beams, columns and slab. The columns were 150×150 mm in width and breadth. 12 mm Φ and 8 mm Φ bar had been used as longitudinal reinforcement and transverse reinforcement (tie bar), respectively. The dimensions of the longitudinal beam (B1) were 150×225 mm and those of the transverse beam (B2) were 150×150 mm. 12 mm Φ bar had been used as longitudinal reinforcement. 8 mm Φ bar was used as stirrups. There was no tie bar (shear reinforcement) in the BC joints. Neither beams nor the columns had any lap joint. Thickness of the slab was 75 mm having one layer of reinforcement in both X and Y directions. Tie and stirrups had standard 90° hook as per BNBC (1993). Two control specimens had also been constructed. Dimensions and detailing of the as built models are shown in Fig. 1. Concrete strength of the samples is shown in Table 1.

Strengthening the joints

The joints were retrofitted in three schemes. In first two schemes, joints were retrofitted by CFRP plate and fabric and in the third scheme joint was retrofitted by introducing tie bars around the column and replacing the concrete by micro-concrete.

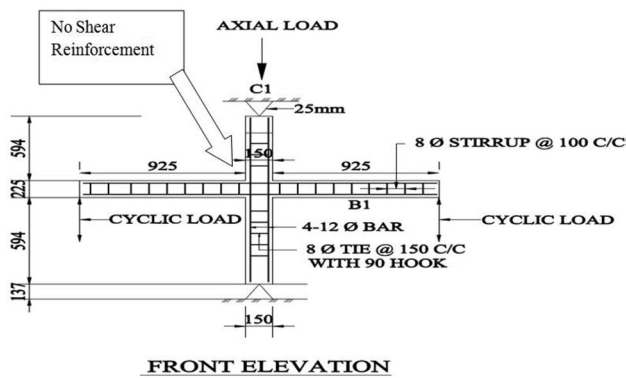


Fig. 1 Dimensions and detailing of models

Table 1 Concrete strength of the samples

Mix no.	Average strength (MPa)	Mix no.	Average strength (MPa)
Con-1	18.31	Fabrics-1	21
Con-2	28.31	Fabrics-2	24.53
Plate-1	15.03	Fabrics-3	33.77
Plate-2	26.8	MCS-1	18.0

First scheme: strengthening by CFRP fabrics

Top and bottom columns were wrapped up to 150 mm from the top of the slab and bottom of the deeper beams, respectively. Beams were wrapped up to 150 mm length in U shape from the face of the column. CFRP wraps is not recommended to use for inside corners and minimum 12 mm radius should be provided for confinement by FRPs. The models had transverse beams at all four sides with slab on top. The beams and column sides were rounded to provide 12 mm radius curvature. The surface of the beams and columns were smoothed by grinding machine and cleaned thoroughly by brush before applying Primer. Hardener and base (1:2 ratios) were mixed thoroughly for 3 min before applying on the prepared surface. This epoxy primer was applied using a brush and dried for 24 h before applying the saturant. The fabrics were cut into 150 mm in width and 300 mm and 450 mm in length. The hardener and the base (1:2 ratios) of the saturant were mixed and applied over the primed surface. CFRP fabric had been pressed on to the saturant applied area by hand first and then was pressed by a surface roller to remove air bubbles. After 30 min another coat of saturant was applied over the carbon fabrics.

Second scheme: strengthening by CFRP plates

In second scheme, the joints had been strengthened by introducing FRP plate into the joint. The concrete from beam at column face, up to 75 mm, were removed to insert the CFRP plates. CFRP plate was cut into pieces of 300 mm in length. Each of the joints was strengthened by four plates. Exposed surfaces were prepared by the grinding machine. Hardener and base (1:2 ratios) of epoxy adhesive had been mixed thoroughly before application. The mixed adhesive was applied on the CFRP plates and pressed over the joint area to squeeze out the mixed adhesive. Additional adhesive had been applied to remove any voids underneath the plate. The joint concrete was replaced by the micro-concrete after 3 days of placing the plates and another two CFRP plates were placed after 7 days of casting by micro-concrete.

Third scheme: strengthening by tie bar and micro-concrete

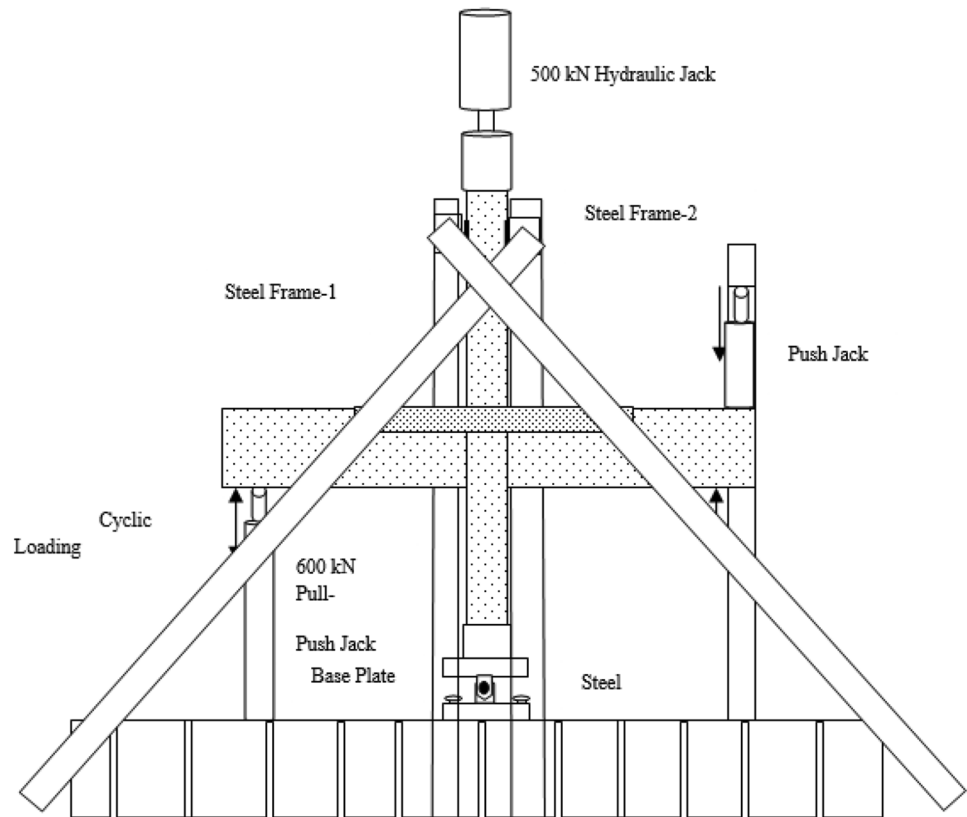
Concrete up to 75 mm from the face of the beam was removed from all sides of the corner joint region. 8 mm Φ tie bars each of 200 mm in length were welded around the column. Later micro concrete was used for the casting.

Experimental setup

The experiment had been carried out in Concrete and Strength of Materials Laboratory of BUET. The models were placed on a steel base plate which had the arrangement of column seat. The base plate was intended to allow column rotation. The base plate was fixed on a steel beam which was fixed with the concrete floor. A hydraulic jack was set to provide axial load on the top of the column. Two sets of steel frame had been designed for this experiment. They were fixed at both side of the column to arrest any horizontal movement of the column. Two manually operated hydraulic jacks were used to provide cyclic loading at the tip of the beams. Total five dial gauges were used to measure the deflection of the beam and columns. First two dial gauges were set near the tip and at the beam-slab joint of the right beam whereas one dial gauge was fixed at the beam-slab joint of the left beam. Another two dial gauges were set at below the top of column and at 10 cm distance from the column-slab joint. Video extensometer was used to measure the rotation of the beam and column joint. Video extensometer had been placed much closed to the joint due to space constrain and location of the steel frame. The experimental setup is shown in Fig. 2.

The strength of BC joints is influenced by the effective confinement. Column axial load increase the confinement. The samples were made from different concrete batches as

Fig. 2 Experimental set up



such their concrete strength had been different. To understand the behavior of all joints under identical condition 10% of the column capacity ($0.1f_c'A_g$) was provided as the axial load. Axial load had been constant throughout the experiment. Axial loads and capacities of the control and strengthened specimens are shown in Table 2.

The static cyclic loading had been provided by two manually operated hydraulic jacks. The load had been controlled by measuring the column drift of the top column. 0.25%, 0.50%, 1% and 2% of the top column drift had been selected to control the load. 5 kN load had been applied while loading and unloading. However, as the jacks were manually operated, unloading could not be maintained at the same rate.

Load deflection response

Load deflection behavior of beam

Deflections of all the samples were measured by five dial gauges and Video Extensometer had been used to measure

the joint and column rotations. The test continued till the left dial gauges reached optimum deflection or the jacks reached their maximum lift capacity. The load deflection behavior of all the beams is similar within the elastic range and exhibits a linear relationship.

Beam of Plate 1 exhibited better ductility than the Con 1. The beam yielded at higher loading than the load corresponding to its plastic yield moment in both forward and reverse loading. Beam of MCS 1 failed much closer to its theoretical yield strength. This may be due to the fact the columns failed earlier than the beams and the test discontinued before determining the beam ultimate strength. Beam of Fabrics 1 deflected less with higher loading in forward loading and showed ductile behavior by deflecting high under the same applied load. Beam failed at higher load than its theoretical strength at the joint (Fig. 3).

In Group B, beam of Plate 2 deflected 73% with 86% loading of the con beam 2 in forward loading while it deflected 4% higher than the control beam with 80% excess load in reverse cycle. Beam of Fabrics 2 deflected 96% with 25% higher loading of the beam of Con 2 in forward loading

Table 2 Concrete strength of the samples

Model no.	Con 1	Con 2	Plate 1	Plate 2	MCS 1	Fabrics 1	Fabrics 2	Fabrics 3
Axial load (kN)	45	65	35	60	42	50	55	75

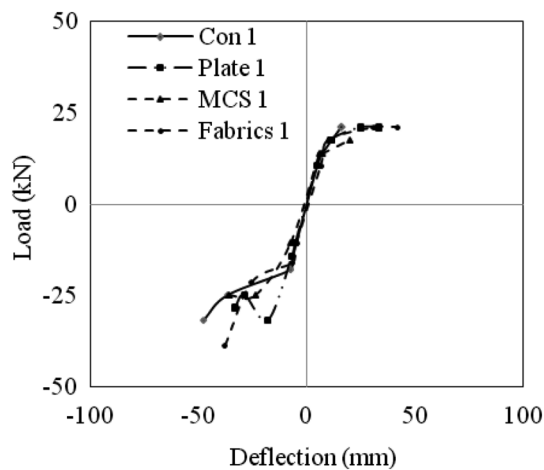


Fig. 3 Load deflection response of beam of Group A

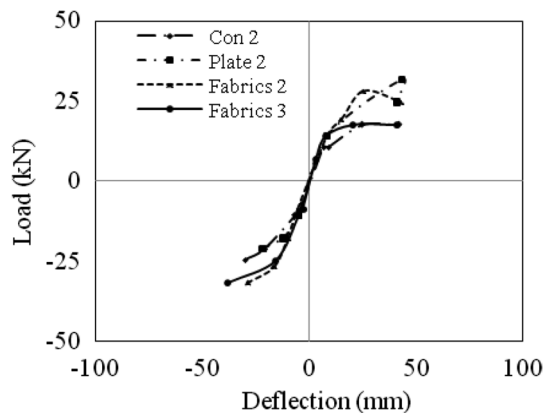


Fig. 4 Load deflection response of beam of Group B

and deflected same amount with 40% higher loading in reverse loading. Beam of Fabrics 3 deflected 27% as high as the control beam in forward loading while loading was 29% higher. In all the cases, the beams yielded at higher loading than their theoretical yield strength (Fig. 4).

Load–deflection behavior of beams is illustrated by hysteresis loops through Fig. 5.

By analyzing the hysteresis loops of the load–deflection, it is found that, within the elastic limit, all the models have non-degrading curve. But in subsequent circles, the loops exhibit stiffness degradation. The characteristics of the hysteresis loops can be analyzed by the slopes of the loading cycles. To evaluate the stiffness of the beams, slope of the forward loading cycles is measured from the load–deflection curve of each cycle. The slope is determined by drawing tangent on forward loading curve. It is found that, the slope gradually decreases as shown in Fig. 6.

Secant stiffness is defined as the ratio of the strength to the maximum displacement. Secant stiffness of the beams

for each load–deflection cycle is measured by considering the maximum load and deflection of both forward and reverse loading and it is found that beam stiffness decreases in each subsequent cycle as shown in Fig. 7.

Load deflection behavior of column

Load deflection response of columns of Group A is presented in the following Fig. 8. Column of Plate 1 experienced enhanced column shear capacity. Column of Plate 1 experienced 6.5% excess column shear force while deflecting 13% less in forward loading and 8% high column shear force while deflecting 93% higher in reverse loading than the column of Con 1. Column of MCS 1 displayed similar behavior of the control model in reverse loading while it deflected 32% high against 17.81% excess loading than that of Con 1 in forward loading. Column of Fabrics 1 deflected same amount against 42.2% excess loading in forward cycle. It deflected 16% more than the column of Con 1 against 46% higher loading. Column of Fabrics 1 experienced high column shear against same deflection compared to the column of Con 1. In all the cases, the columns experienced high shear than their theoretical yield strength except MCS 1 where in later case the column failed at its yield limit.

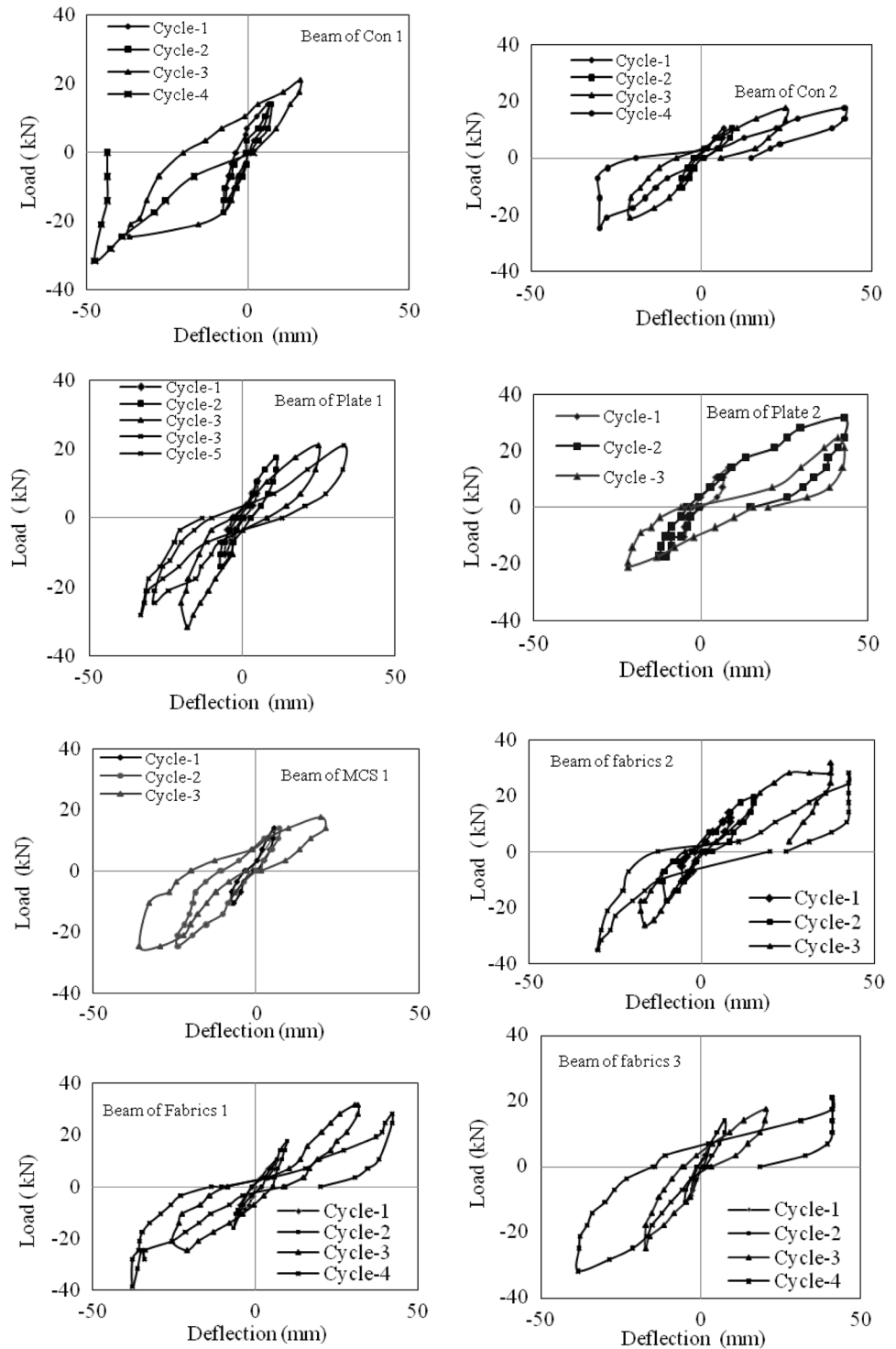
The load–deflection response of columns of Group B is shown through Fig. 8. Column of Plate 2 deflected 87% with 84% loading of the column of Con 2 in forward loading cycle. It experienced 19% higher column shear force than that of Con 2 while deflected only 48.6% of the Column of Con 2 in reverse loading. In forward loading, Column of Fabrics 2 experienced 52% higher shear force than that of Con 2 with the same deflection in forward loading. The column experienced maximum 84% shear force while deflecting 43.4% of the same column of Con 2 in forward loading. The same column experienced column shear 22.7% higher than that of column of Con 2 while deflecting 9.5% more than the same column. Column of Fabrics 3 deflected 7.5% higher than column of Con 2 against 13.3% excess loading in forward cycle but the same column deflected 5.7% higher against 19.1% higher loading in reverse loading cycle. In all the cases, the columns experienced higher shear forces than their theoretical strength (Fig. 9).

The behavior of the columns can be analyzed by the load–deflection hysteresis loops plotted for each cycle. Hysteresis loops for the columns are illustrated in the following Fig. 10.

Slope of the load–deflection cycle is determined to evaluate the magnitude of stiffness degradation of the column. The slope is determined as it was determined for beams. The slopes of the load–deflection cycles of the columns of Group A and B are illustrated by Fig. 11 and 12.

Column secant stiffness for each cycle is measured by considering maximum applied moment against maximum

Fig. 5 Load deflection response of beam



deflection. The computed stiffnesses are illustrated by Fig. 13 and 14.

The slopes and the secant stiffness of the column decreased with the commencement of cycles. The column shear had been measured indirectly from the load applied at the tip of the beam. Upon failure, beams were unable to transfer load on the column. This led to increased column

shear without deflection resulting in higher slope and stiffness in subsequent cycles. The rate of losing stiffness in subsequent cycles indicates the collapse behavior of the member. Percentage of initial stiffness of the column are shown Fig. 15. In Group A, Plate 1 kept higher rate of initial stiffness compared to Con 1 at higher stage of loading. Considering the maximum load provided in each cycle, columns

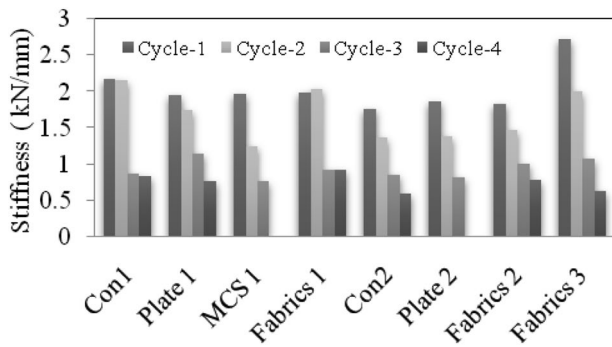


Fig. 6 Forward slope of load deflection cycle of beams

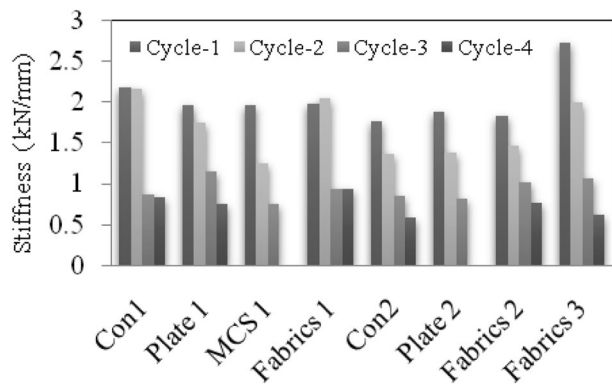


Fig. 7 Stiffness of beams

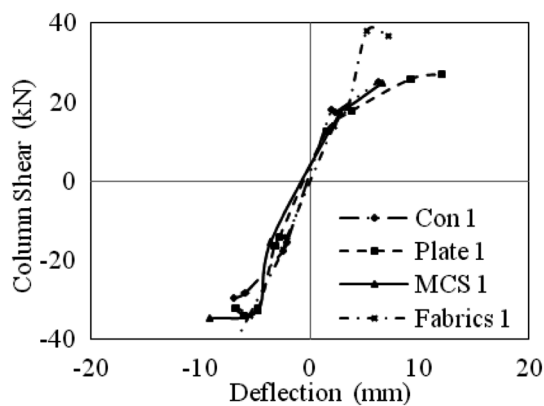


Fig. 8 Load deflection response of column of Group A

of MCS 1 and Fabrics 1 retained high initial stiffness compared to the column of Con 1. In Group B, considering the maximum load provided in each cycle, columns of Plate 2, Fabrics 2 and 3 retained high initial stiffness compared to the column of Con 2.

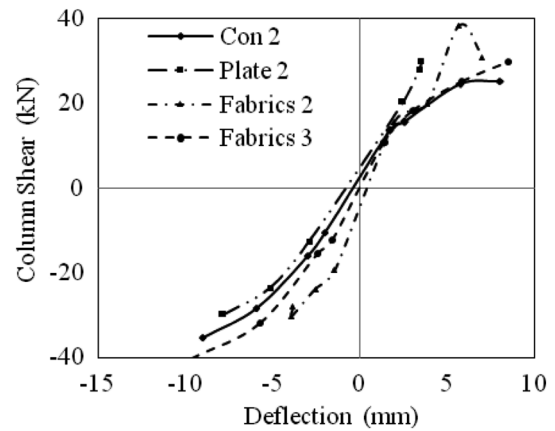


Fig. 9 Load deflection response of column of Group B

Load deflection behavior of column

Rotation experiences by the joints in each cycle depend on the magnitude of the applied moment. Rotations of the beams and columns at the joint against corresponding loading (applied moment) were measured and evaluated by Video Extensometer. Maximum load and corresponding rotation had been found by analyzing the computer output.

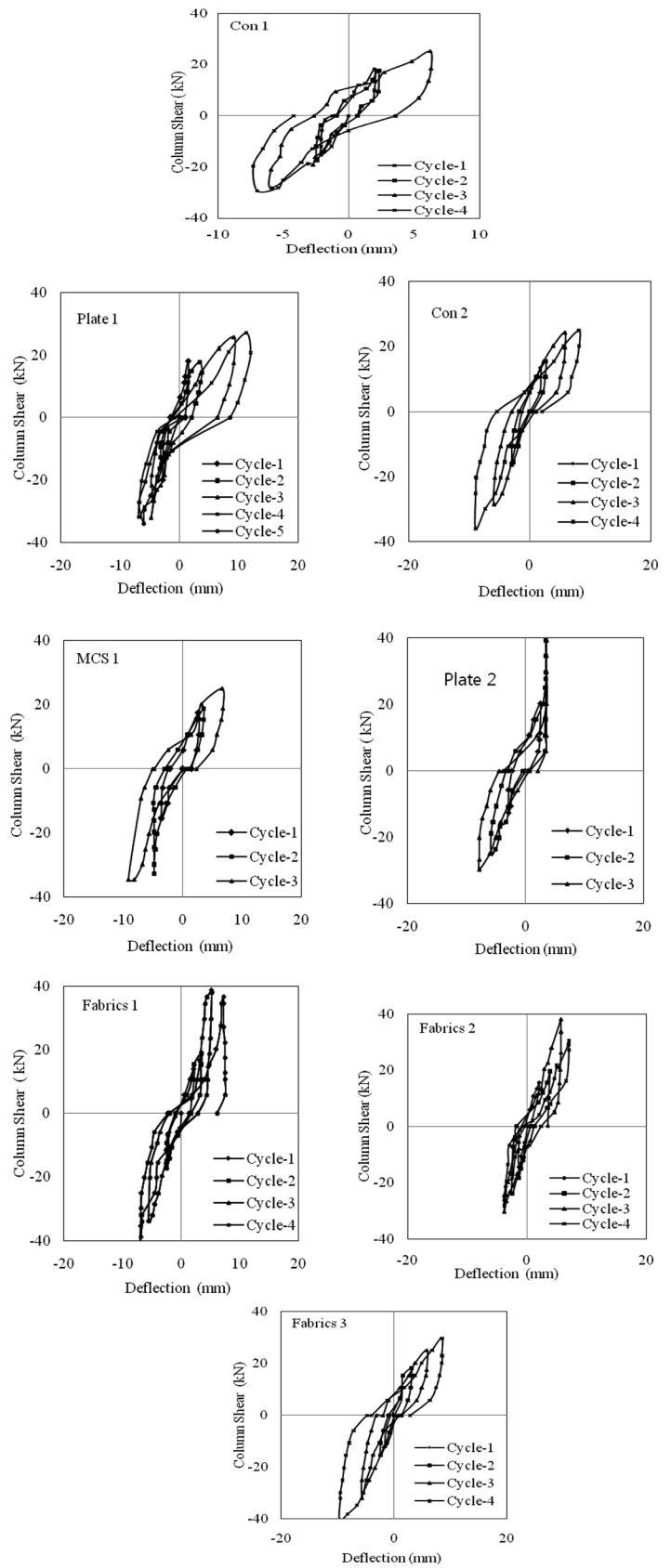
Applied maximum moment and corresponding beam joint rotations of Group A are shown in the following Fig. 16 Beam joint of Con 2 rotated 53.4% more against 22.4% excess loading than that of Con 1 in forward cycle whereas the same beam joint rotated further 75% against the same loading compared to the joint of Con 1. $M-\Phi$ curve of both the joint indicates that the ductility increases with the increased concrete strength. Rotational ductility of Con 1 was 3.45 whereas it was 6.45 for Con 2.

Joint of Plate 1 rotated 86% of the Con joint 1 while applied load was 16.1% higher in forward loading. The same joint rotated 109% higher against 8% excess loading compared to the same control joint. Joint of MCS 1 rotated additional 46.5% when the applied moment was 17.8% higher and it rotated further 89% against the same applied moment in reverse loading compared to the Con 1 joint. The joint of Fabrics 2 rotated 32.3% more against 46% higher applied moment in forward loading compared to Con 1 joint. The same joint rotated additional 45.5% against 42.2% excess loading in comparison to Con joint 1.

Applied maximum moment and the corresponding rotation of the joints in each cycle of Group B are illustrated in the following Fig. 17.

Joint of Plate 2 rotated 46% of the joint of Con 2 in forward loading while it is subjected to 83% load of the control joint. It rotated 70% of the control joint in reverse loading against 74% excess load of the control joint 2. Joint of Fabrics 2 rotated the same against 52.5% excess load of the

Fig. 10 Load deflection response of column



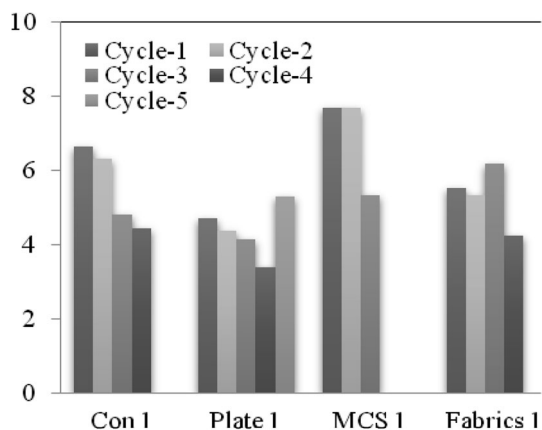


Fig. 11 Slope of load deflection curve o forward loading (Group A)

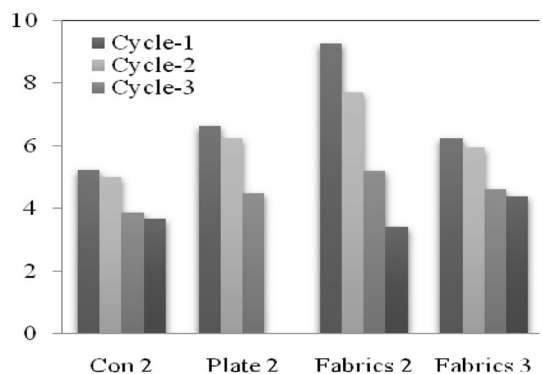


Fig. 12 Slope of load deflection curve o forward loading (Group B)

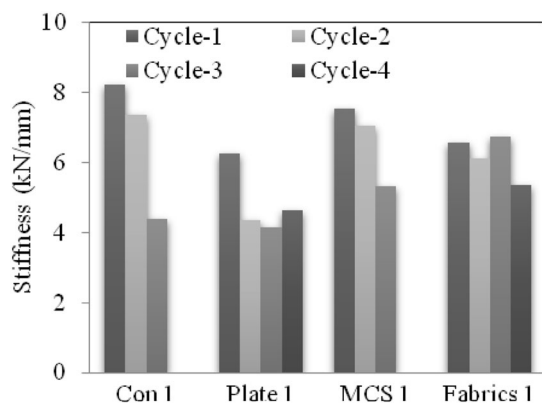


Fig. 13 Column stiffness (Group A)

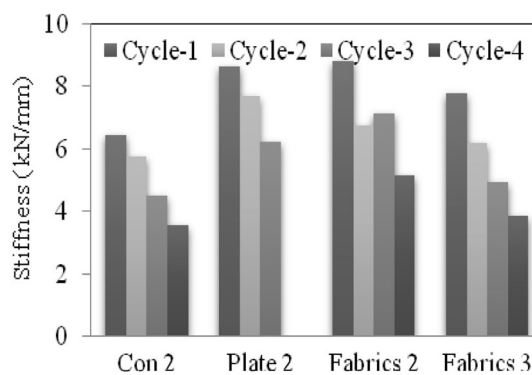


Fig. 14 Column stiffness (Group B)

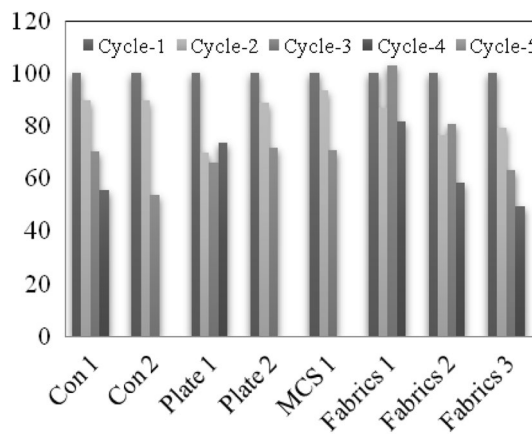


Fig. 15 Percentage of initial column stiffness (Group A and Group B)

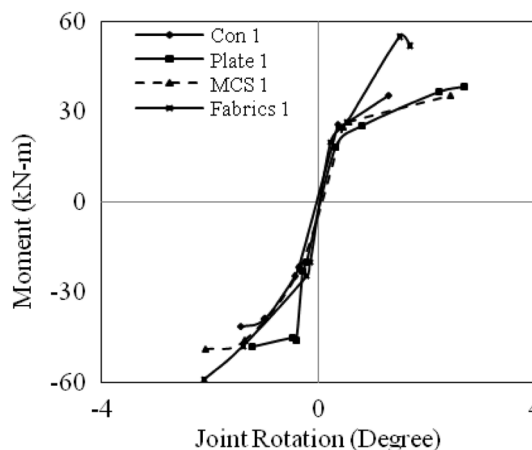


Fig. 16 Applied moment versus rotation of joint (Group A)

control joint in reverse cycle. The same joint had 38% rotation of the control joint in forward loading while it was subjected to 78% load of the control joint. Fabrics 3 joint rotated 75% of the control joint 2 against 11.78% excess loading in

forward loading cycle. The rotation of the same joint was 21.4% higher against 19% excess loading in reverse loading.

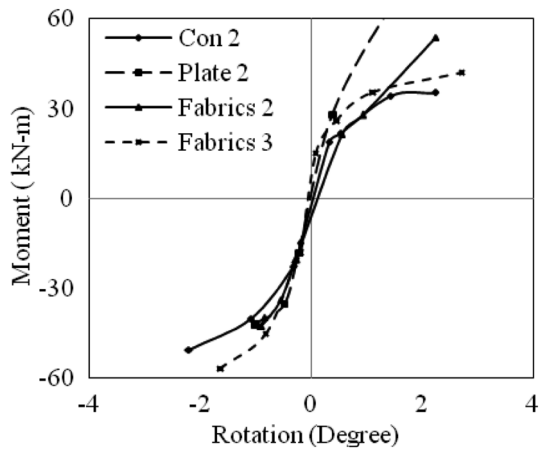


Fig. 17 Applied moment versus rotation of joint (Group B)

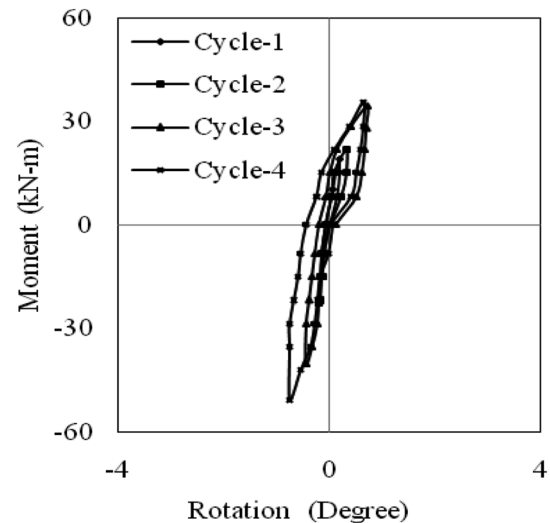


Fig. 19 Rotation of column joint of Con 2

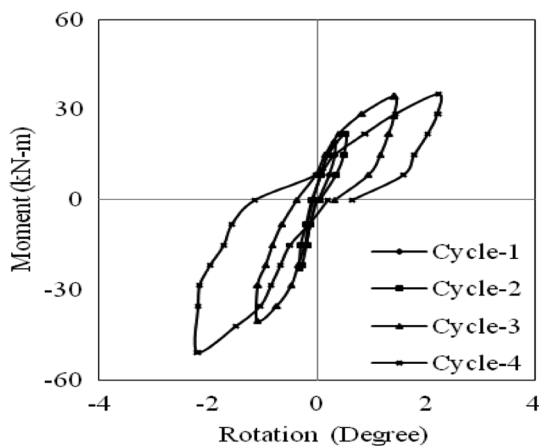


Fig. 18 Rotation of beam joint of Con 2

Hysteresis loops of Con 2, Plate 2, MCS 1, and Fabrics 3 column and beam joints are shown through Figs. 18, 19, 20, 21, 22, 23, 24, 25, 26, 27, 28, 29, 30, 31, 32 and 33.

It is found that the column and joint rotate equally for all the models within the elastic limit but their relative rotations are different in subsequent cycles. The rotation of the column and joints are plotted together to evaluate their relative rotation. The magnitude of maximum rotation experienced by the beam joints in each cycle are illustrated through Figs. 34 and 35.

Rotational stiffness means the moment required to cause unit rotation. High stiffness means high resistance to deflection. Secant Rotational Stiffness of the joint is computed by averaging the maximum rotation against the applied maximum moment.

Rotational stiffness of Group A and B are illustrated through Figs. 36 and 37. The rotational stiffness joint decreased with the commencement of the cycles for all samples in Group A and B. Plate 1 exhibited high

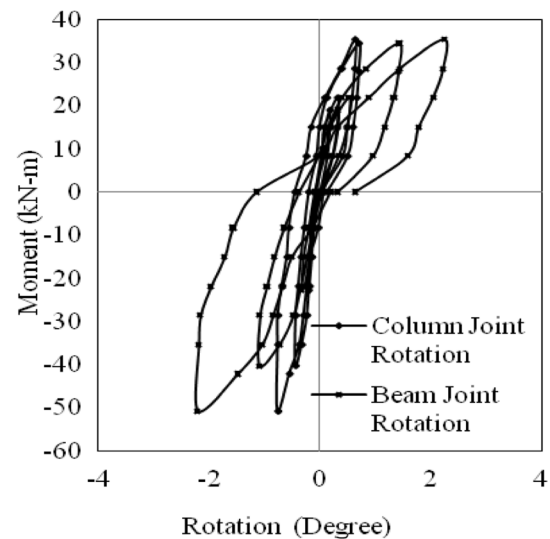


Fig. 20 Relative rotation of beam and column joint of Con 2

rotational stiffness compared to the joint of Con 1 considering the concrete strength. Rotational stiffness of the joint of MCS 1 was less compared to stiffness of the joint of Con 1.

In Group B, rotational stiffness of the joint of Plate 2 was higher than that of the joint of Con 2 in all cycles of loading. Rotational stiffness of the joint of Fabrics 2 was slightly less compared to the rotational stiffness of the joint of Con 2 considering the concrete strength. Rotational stiffness of the joint of Fabrics 3 is higher than that of the control joint considering the concrete strength for all the cycles (Fig. 38).

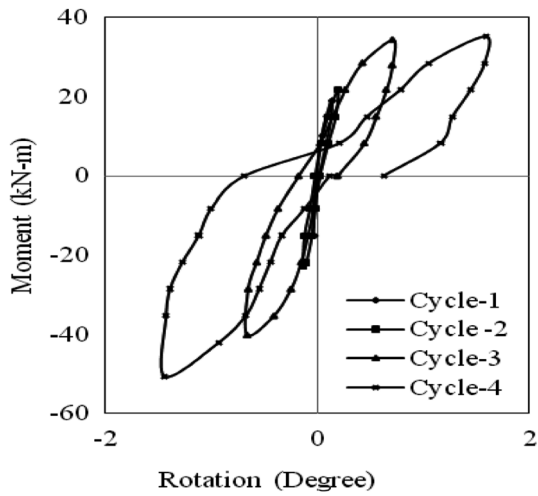


Fig. 21 Difference of beam and column joint rotation of Con 2

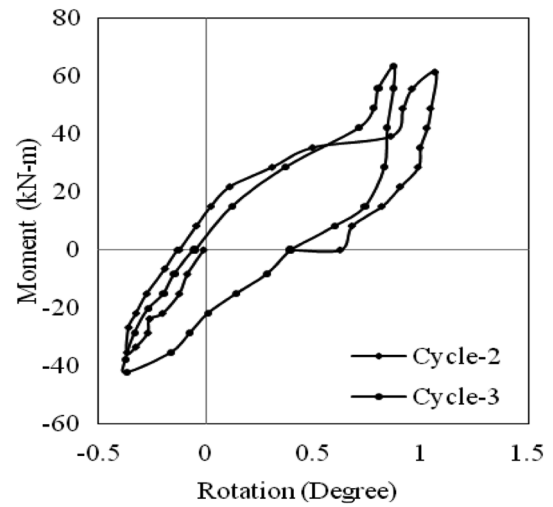


Fig. 23 Rotation of column joint of Plate 2

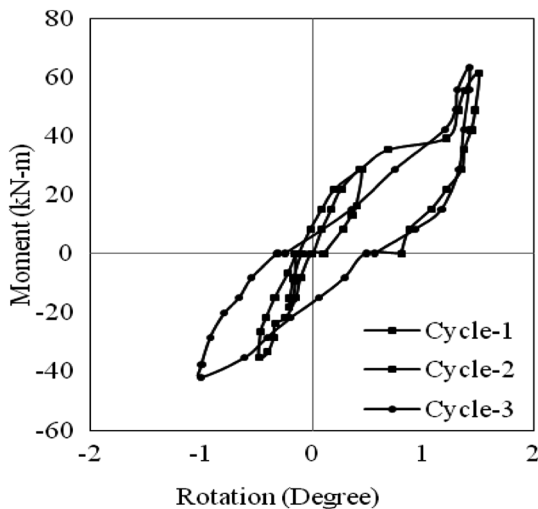


Fig. 22 Rotation of beam joint of Plate 2

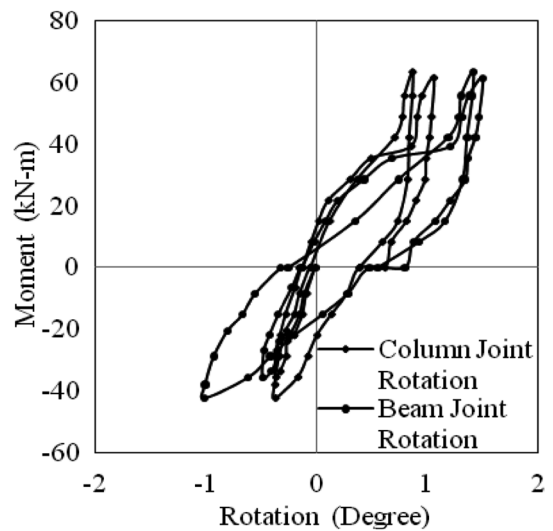


Fig. 24 Relative rotation of column and beam joint of Plate 2

It is normal for the structural member to lose some stiffness under cyclic loading, but excessive loss of stiffness can lead to a collapse. Percentage of initial stiffness of the joints in subsequent cycles is computed to measure the rate of loss of stiffness from the initial value and the values are illustrated in Fig. 37. The joints of Con 1 and Con 2 retained 43% and 29% of the initial stiffness. Plate 1 and 2 retain 37% and 59% of the initial stiffness. Fabrics 1, 2 and 3 retain 29%, 60% and 18.86% of the initial stiffness.

Conclusions

Behavior of the interior joints under cyclic loading, both control specimens and the retrofitted ones, were investigated based on the performed test result. Following conclusions are drawn based on the experiment and analysis of the results:

- (a) Diagonal cracks occurred under cyclic loading in interior joints which lack in shear reinforcement. Diagonal cracks of such specimen traveled to transverse beams at higher stage of loading and caused the transverse beam to fail.

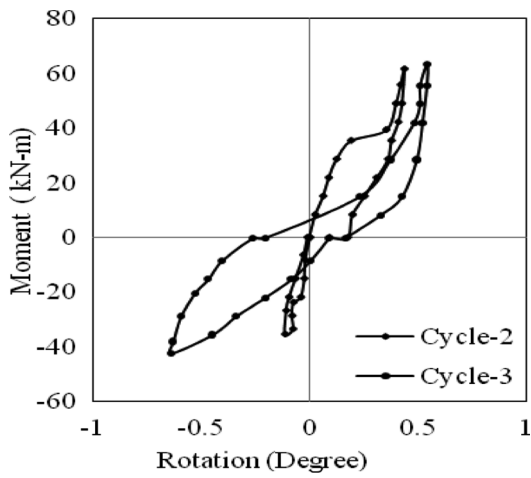


Fig. 25 Difference in beam and column joint rotation of Plate 2

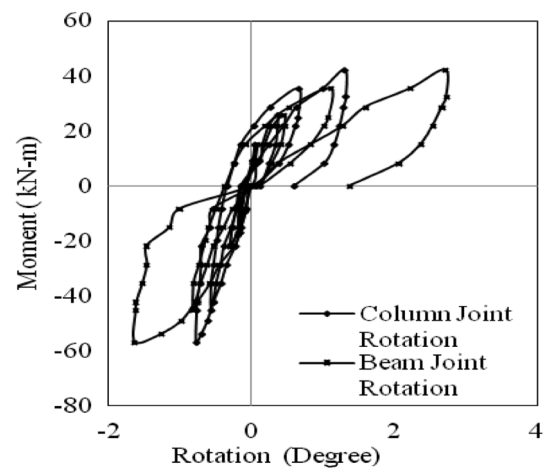


Fig. 28 Rotation of beam and column joint of Fabrics 3

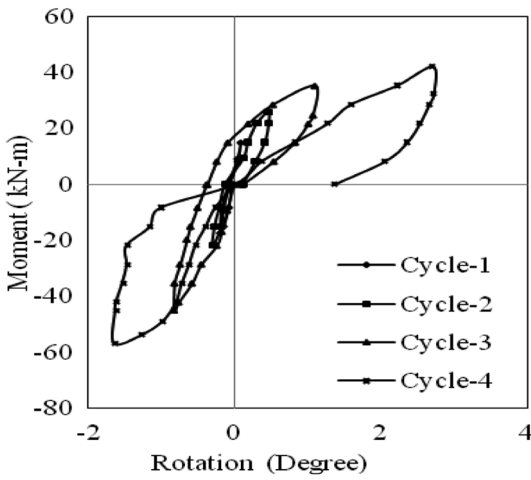


Fig. 26 Rotation of beam joint of Fabrics 3

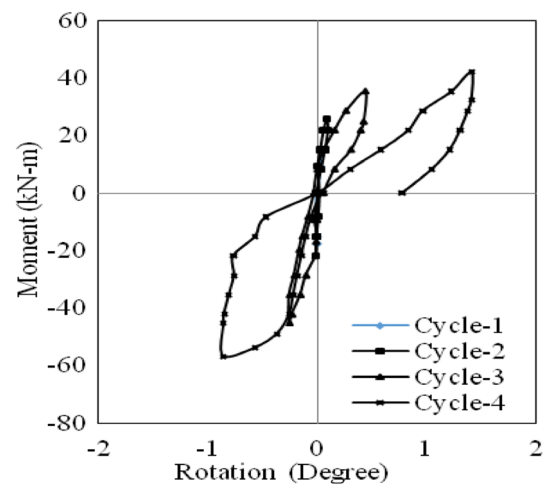


Fig. 29 Difference in beam and column joint rotation of Fabrics 3

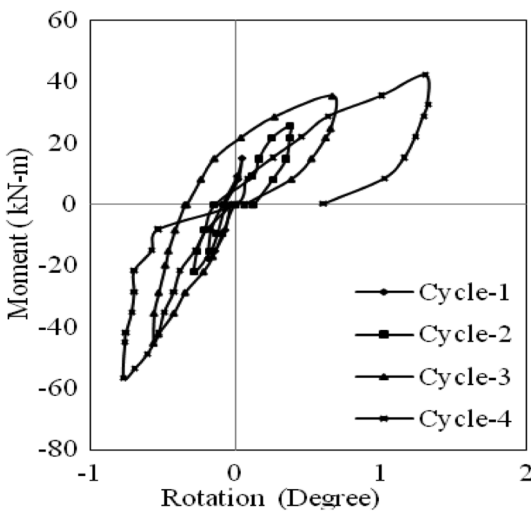


Fig. 27 Rotation of column joint of Fabrics 3

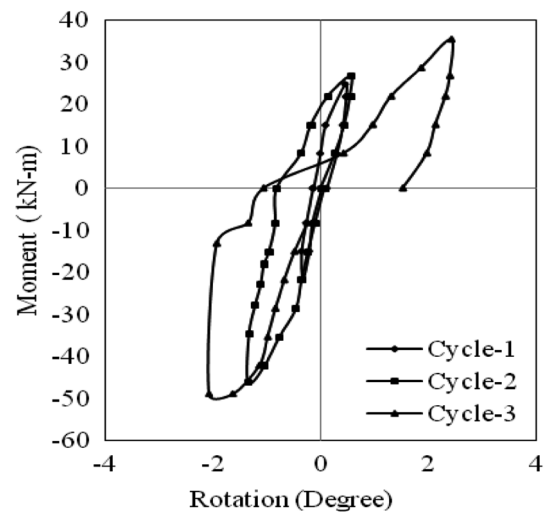


Fig. 30 Rotation of beam joint of MCS 1

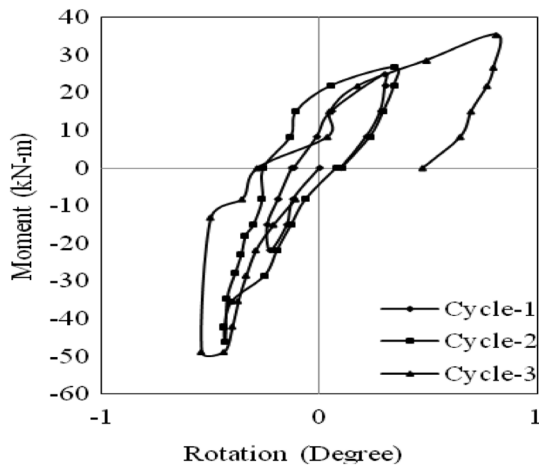


Fig. 31 Rotation of column joint of MCS 1

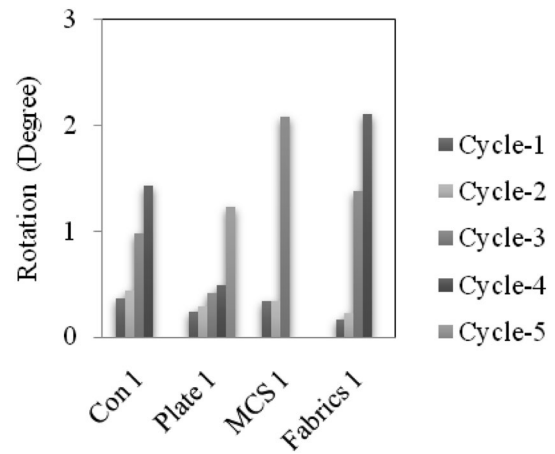


Fig. 34 Rotation of beam joints in forward cycle (Group A)

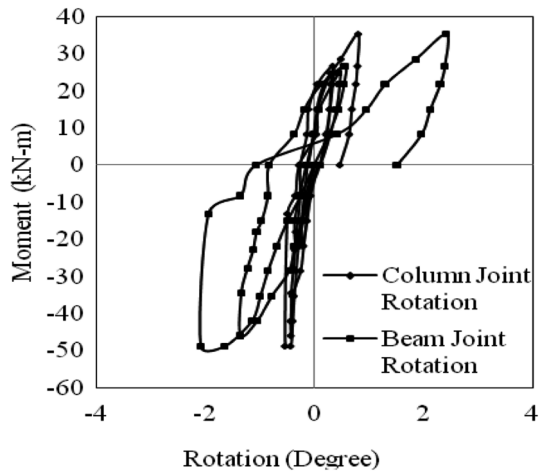


Fig. 32 Relative rotation of beam and column joint of MCS 1

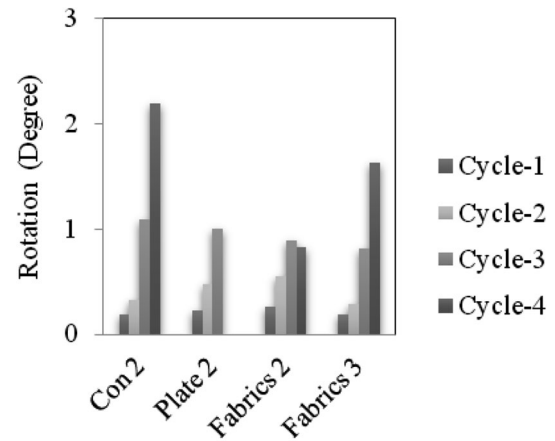


Fig. 35 Rotation of joints in forward cycle (Group B)

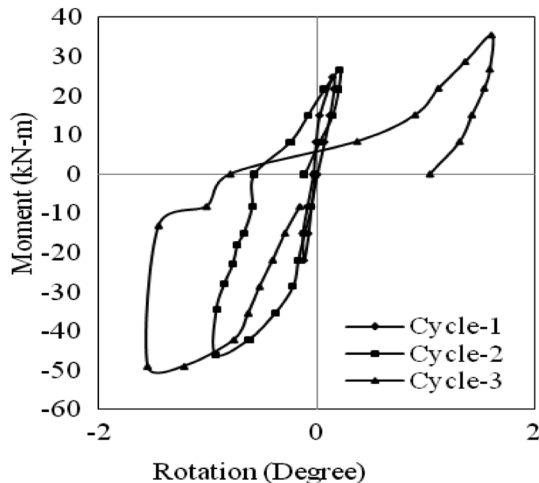


Fig. 33 Difference in beam and column joint rotation of MCS 1

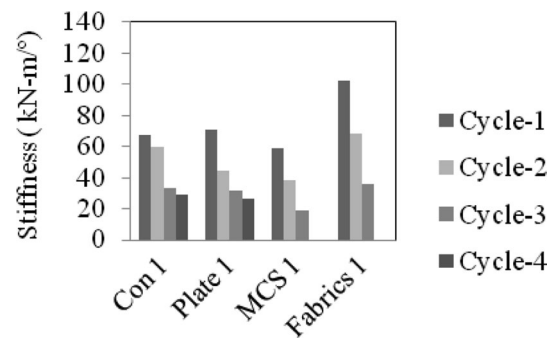


Fig. 36 Joint stiffness of Group A

(b) Ductility of beams, columns and joints increased with increased concrete strength. Rotational ductility of the joints increased 2.5–2.75 times by increasing 54% of the concrete strength.

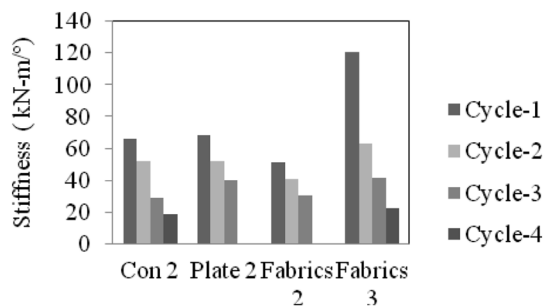


Fig. 37 Joint rotational stiffness of Group B

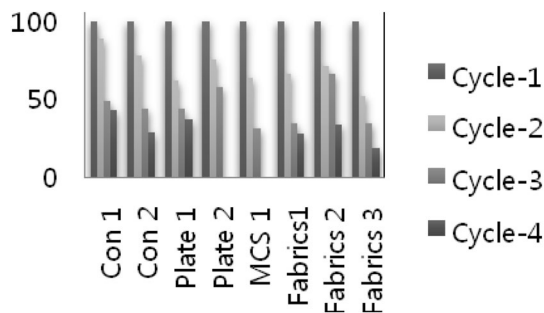


Fig. 38 Percentage of initial rotational stiffness

- (c) Stiffness of the joints decreased gradually under cyclic loading. But, Stiffness of the joint did not degrade at the same rate for all the retrofitted samples.
- (d) The rotational capacity of the joints can be increased by strengthening the BC joints by CFRP plates. Rotational stiffness of these joints was higher than that of the control models. Rotational stiffness of these joints also decreased gradually. From $M-\Phi$ curve, it is found that BC joints strengthened by CFRP plates show ductile behavior.
- (e) CFRP plate is effective in resisting diagonal crack travelling to transverse beams. Diagonal crack traveled up to the CFRP plate and changed their direction. Beams from both the models, failed at the plate-beam joints. It can be concluded that location of plastic hinge may be altered by altering the length of the plate.
- (f) Moment capacity of the joints can be enhanced by additional tie bar in the joint and micro-concrete depending on the initial concrete strength. Joint retrofitted by micro-concrete and additional tie bar underwent large deformation before failure exhibiting ductile behavior of the joint.
- (g) Joints can be strengthened by CFRP fabrics. Moment capacities of the joints strengthened by CFRP fabrics were higher against the same rotations compared to the control models.
- (h) Joints strengthened by CFRP fabrics undergo greater deformation than the control joints. Joints strengthened by CFRP fabrics exhibited better ductile behavior than the control models.
- (i) The mode of failure may be shifted from column to beam by strengthening joints by CFRP fabrics. Column shear and flexural capacity can be increased by CFRP wrapping.
- (j) Micro-concrete and concrete have good bonding strength as micro-concrete was used for strengthening joints by CFRP plates and additional tie bar. Micro-concrete and concrete joints failed at higher stage of loading and associated with plate debonding.

Compliance with ethical standards

Conflict of interest On behalf of all authors, the corresponding author states that there is no conflict of interest.

References

- ACI-352R-76. (1976). Recommendations for design of beam-column joints in monolithic reinforced concrete structures. In 1976 (Vol. 73, pp. 375–393). American Concrete Institute.
- Akguzel, U., & Pampanin, S. (2011). Assessment and design procedure for the seismic retrofit of reinforced concrete beam-column joints using FRP composite materials. *Journal of Composites for Construction*, 16(1), 21–34.
- Al-Musallam, T. H., & Al-Salloum, Y. A. (2007). Seismic response of interior RC beam-column joints upgraded with FRP sheets. II: Analysis and parametric study. *Journal of Composites for Construction*, 11(6), 590–600.
- Bai, J.-W., Center, M.-A. E., & Hueste, M. B. (2003). *Seismic retrofit for reinforced concrete building structures*. College Station: Mid-America Earthquake Center, CM-4, Texas A&M University.
- Beydokhty, E. Z., & Shariatmadar, H. (2016). Behavior of damaged exterior RC beam-column joints strengthened by CFRP composites. *Latin American journal of solids and structures*, 13(5), 880–896.
- BNBC. (1993). Bangladesh national building code (BNBC). Dhaka, Bangladesh.
- Ichinose, T. (1991). Interaction between bond at beam bars and shear reinforcement in R/C interior joints. *Special Publication*, 123, 379–400.
- Li, B., & Kai, Q. (2010). Seismic behavior of reinforced concrete interior beam-wide column joints repaired using FRP. *Journal of Composites for Construction*, 15(3), 327–338.
- Mahini, S. S., & Rounagh, H. R. (2007). A new method for improving ductility in existing RC ordinary moment resisting frames using FRPs. *Asian Journal of Civil Engineering (Building and Housing)*, 8(6), 581–595.
- Mayfield, B., Kong, F.-K., Bennison, A., & Davies, J. C. T. (1971). Corner joint details in structural lightweight concrete. *ACI Journal*, 68(5), 366–372.

- Mukherjee, A., & Joshi, M. (2005). FRPC reinforced concrete beam-column joints under cyclic excitation. *Composite Structures*, 70(2), 185–199.
- Murshed, A. (2011). *Seismic performance of soft storey structures retrofitted with FRP wraps*. Dhaka: Bangladesh University of Engineering and Technology.
- NZS 3101:1982. (1982). New Zealand standard code of practice for the design of concrete structures. NZS 3101, Standard Association of New Zealand.
- Obaidat, Y. T., Abu-Farsakh, G. A., & Ashteyat, A. M. (2019). Retrofitting of partially damaged reinforced concrete beam-column joints using various plate-configurations of CFRP under cyclic loading. *Construction and Building Materials*, 198, 313–322.
- Pantelides, C. P., Clyde, C., & Reaveley, L. (2000). Rehabilitation of R/C building joints with FRP composites. In *12th world conference on earthquake engineering, Auckland, New Zealand*.
- Pohoryles, D., Melo, J., Rossetto, T., Varum, H., & D'ayala, D. (2015). Experimental investigation on the seismic FRP retrofit of realistic full-scale RC beam-column joints. In *Improving the seismic performance of existing buildings and other structures 2015* (pp. 619–631).
- Prota, A., Nanni, A., Manfredi, G., & Cosenza, E. (2004). Selective upgrade of underdesigned reinforced concrete beam-column joints using carbon fiber-reinforced polymers. *Structural Journal*, 101(5), 699–707.
- Sezen, H. (2012). Repair and strengthening of reinforced concrete beam-column joints with fiber-reinforced polymer composites. *Journal of Composites for Construction*, 16(5), 499–506.
- Sharma, A., Genesio, G., Reddy, G., Eligehausen, R., Pampanin, S., & Vaze, K. (2010). Experimental investigations on seismic retrofitting of reinforced concrete beam-column joints. In *14th symposium on earthquake engineering, 2010* (paper no. A007).
- Shiohara, H., & Kusuhara, F. (2010). An overlooked failure mechanism of reinforced concrete beam-column joints. In *Proceedings of the 9th NCEE, July, 25–29*.
- Zgür Yurdakul, Ö., & Avşar, Ö. (2015). Structural repairing of damaged reinforced concrete beam-column assemblies with CFRPs. *Structural Engineering and Mechanics*, 54(3), 521–543.

Publisher's Note Springer Nature remains neutral with regard to jurisdictional claims in published maps and institutional affiliations.